

Sequestration of Heavy Metals From Coal Wash Water Using Biochar From Pyrolysis of Morula Shells

Lame Elsie Othugile¹, Tumeletso Lekgoba^{1*}, Freeman Ntuli^{1,2}

¹Department of Chemical, Materials and Metallurgical Engineering, Botswana International University of Science and Technology, Palapye, BOTSWANA

²Department of Chemical Engineering Technology, University of Johannesburg, Doornfontein, Johannesburg, SOUTH AFRICA

*Corresponding Author: lekgobat@biust.ac.bw

Citation: Othugile, L. E., Lekgoba, T. and Ntuli, F. (2022). Sequestration of Heavy Metals From Coal Wash Water Using Biochar From Pyrolysis of Morula Shells. *European Journal of Sustainable Development Research*, 6(1), em0173. <https://doi.org/10.21601/ejosdr/11377>

ARTICLE INFO

Received: 30 Jun. 2021

Accepted: 2 Oct. 2021

ABSTRACT

Biomass is a source of low-cost adsorbents used in the removal of contaminants. In this study, shells from an indigenous tree in Southern Africa called Morula were pyrolyzed to produce biochar that was used to sequester heavy metals from coal wash water. The produced biochar was activated using hydrochloric acid (HCl) and parameters such as the cation exchange capacity (CEC), point of zero charge (pH_{zc}), elemental composition, mineral composition, proximate analysis and surface functional groups were determined. Batch adsorption experiments were carried out at 150 rpm for 60 min and 25 °C at different metal ion concentrations and adsorbent dosages. The metal ions of interest were Zn, Ni and Fe and it was found that Fe recorded higher removals for both raw and activated biochar. Generally higher removals were noticed for both raw and activated at lower dosages (0.2 – 1.0 g/100 mL) and lower metal ion concentration (between 40 and 60 ppm) while lower removals were found at higher dosages (1 – 5 g/100 mL) and higher metal ion concentrations (between 400 – 600 ppm).

Keywords: adsorption, biochar, coal wash water, Morula Shells, sequestration

INTRODUCTION

Water pollution is a serious global issue which adversely affects our lives and studies show that it is expected to worsen in the coming decades (Ali and Gupta, 2007). Over the years, the main source of health concerns in water has been microbial contaminants. But with time, it was discovered that chemical contaminants also contribute to pollution of water sources after discovery of analytical methods to measure these contaminants (Sharma and Bhattacharya, 2017). These include anionic substances (nitrates, sulphates, chlorides, fluorides and phosphates), toxic metals including heavy metals and organics such as pesticides, herbicides, fungicides and insecticides together with dyes and hydrocarbons (Sen and Gomez, 2011). These contaminants are contained in effluents from different industrial activities such as manufacture of cosmetics, pharmaceuticals, fertilisers, food, textiles, steel and mining industries (Cao et al., 2019). Among these pollutants, heavy metals such as Fe, Cu, Cd, Pb, Co, Ni, Hg and As are classified as harmful due to their toxicity to the environment and non-biodegradability and their presence in water causes bioaccumulation in living organisms. Even though some are essential for micronutrients in the soil from underground water, some cause damage to the nervous system and internal organs in human beings if found in certain concentrations in

potable water (Abdullah, 2013). The further increase in population growth, industrialization, domestic, mining and agricultural activities worsen the situation. In response to this, treatment technologies such as ion exchange, chemical precipitation, adsorption and membrane technologies have been developed by these industries to treat wastewater prior to its disposal to the environment (Malaviya and Singh, 2011). Research on adsorption was unearthed by the desire to achieve zero pollution and a green technology as it was identified as environmentally friendly due to application of clean adsorbent materials especially biochars.

The aim of this research was to utilize biochar produced from the pyrolysis of morula shells at 600 °C to sequester heavy metal ions from aqueous solutions. Morula (*Sclerocarya Birrea*) is a naturally occurring fruit tree found in abundance in Southern African countries such as Botswana, Zimbabwe, Zambia, Namibia and South Africa (Wynberg et al., 2014). Even though this is a seasonal fruit, the shells are readily available throughout the year and often disposed as waste material and hence its recent consideration for use as a low-cost adsorbent. The present study involved investigating the effect of both raw and modified biochar on the removal of Zn, Ni and Fe from aqueous solutions.

MATERIALS AND METHODS

Materials

Wastewater collected from a local coal mine was used for this study. A dilution ratio of 1:10 with distilled water was used to prepare the lower ion concentration wastewater with the objective of understanding the behaviour of the biochar when metal ion concentrations are reduced. The samples were then acidified with small amount of nitric acid to preserve the water samples from forming metal compounds. Morula shells were collected from a nearby tree and pyrolyzed using a batch pyrolysis pilot plant. 2 M HCL was used to activate the biochar produced. Sodium acetate (NaCH_3CO_2), ammonium acetate ($\text{NH}_4\text{CH}_3\text{CO}_2$) and ethanol ($\text{C}_2\text{H}_5\text{OH}$) were used for determination of cation exchange capacity using the ammonium acetate displacement method. 0.1 M NaOH and 0.1M HNO_3 were used to adjust the pH of the solution while 0.01 M of KNO_3 was used as solution for point of zero charge determination. All chemical reagents were of analytical grade and were all supplied by Rochelle Chemicals.

Apparatus

Inductively Coupled Plasma- Optimal Emission Spectrometry (ICP-OES) iCAP (Thermo Scientific 7000 series) was used for metal ion analysis. Handheld XRF Olympus Delta Premium-50 kV was used for elemental composition analysis of both raw and activated biochar. A Malvern Mastersizer 300E – Hydro laser particle analyser was used for particle size analysis while the proximate analysis was done using Leco TGA 701 Thermo-Gravimetric Analyser. Functional group characterization was done using the Raman Spectrometer (Horiba Scientific). VWR Incubating shaker was used for conducting the batch adsorption experiments and the Drawell DW-XRD-Y3000 was used for mineral identification.

Cation Exchange Capacity (CEC)

About 0.20 g of biochar was leached five times with 20 mL of deionized water to reduce any interference with soluble salts. Then, the biochar was leached with 20 mL of 1 M sodium acetate five times to dissolve sodium ions on the exchangeable sites. After that, the sample was washed with 20 mL of ethanol five times to remove the excess Na^+ . Afterwards, the Na^+ on the exchangeable sites of the biochar was displaced by 20 mL of 1 M ammonium acetate (pH 7) five times, and the CEC of the biochar was calculated from the Na^+ displaced by NH_4^+ using Equation 1.

$$CEC = \frac{C_{Na} \times V}{MM_{Na} \times M_{ad}} \quad (1)$$

Where, CEC is the Cation Exchange Capacity in meq/100g of adsorbent, C_{Na} is the concentration of Na^+ in mg/L, V is the volume of solution in mL, MM_{Na} is the molar mass of Na in g/mol and M_{ad} is the mass of the adsorbent used in g.

Point of Zero Charge (pH_{ZC})

The point of zero charge for morula biochar was determined by adding 0.1 g of biochar to a series of 100 mL conical flasks; 5 flasks containing 0.01 M of KNO_3 and 5 flasks containing distilled water. The pH of both solutions was varied from 2.5 to 10.5 with increments of 2.0 using either 0.1 M

NaOH or 0.1 M HNO_3 . The flasks were then placed in a mechanical shaker at room temperature and pressure and rotated for 60 minutes at 120 rpm. The pH values of the suspensions were then measured. The pH of the suspension was represented as a function of the initial solution pH. The initial pH of the solution (pH_i) was plotted against the difference between the initial and final pH values ($\Delta\text{pH} = \text{pH}_i - \text{pH}_f$) from which the pH_{ZC} was estimated at pH_i where the graph cuts the x-axis at $\Delta\text{pH} = 0$.

Activation of the Biochar

Chemical activation was be done using hydrochloric acid (HCl). The sample was divided into two 50 g samples for the process. The ratio of impregnation was 1 g of sample to 20 mL acid (Hayashi et al., 2000). 50 g of char was added to 1000 mL of 2 M HCl in water and an overhead stirrer was used at 200 rpm for 2 h for proper mixing then heated at 110°C for 4 h. After the mixture was cooled, it was then filtered with 6 μm filter papers. To remove the acid, the filtered sample was washed first with distilled water and stirred at 150 rpm for 30 min for proper washing then filtered again. The pH of the filtrate was observed to be 2.65 which showed that the acid was not washed off. Thus, the sample was soaked in 2% NaHCO_3 till any residual acid left has been removed and pH was tested again to be 8.42. Lastly, the char was washed with deionized water until the pH was stable around 5.85 (initial pH of char). Then the sample was washed with distilled water again to remove any base left. The activated biochar was the filtered again and left to dry overnight.

Adsorption Experiments

Different adsorbent dosages were used for the two different adsorbate solutions for both raw and activated biochar. 1.0 – 5.0 g of biochar was added to different 100 ml solutions of the coal wash water of higher metal ion concentrations and 0.2 – 1.0 g of biochar was used for lower metal concentrations. The solution was then agitated at 25°C and 150 rpm for 60 min using VWR incubating shaker. After shaking, the solutions were then filtered using membrane filters of pore size 0.45 μm and the filtrate was acidified with 1 drop of nitric acid to preserve the sample then stored at room temperature awaiting metal analysis using ICP-OES. After metal analysis, the removal percentages were calculated using the Equation 2.

$$\% \text{Removal} = \frac{C_o - C_f}{C_o} \times 100\% \quad (2)$$

Where C_o and C_f are the concentrations of metal ions before and after adsorption in mg/L

RESULTS AND DISCUSSION

Characterization of the Adsorbent

Mineral Composition (XRD)

In a diffractometric pattern, sharp peaks represent crystalline phases while amorphous phases are shown by broad peaks (Kapur and Mondal, 2014; Lekgoba et al., 2020). **Figure 1** shows that morula biochar is amorphous and both activated and raw fly ash are showing a similar diffractometric pattern which suggests that the activation of morula char did not effect

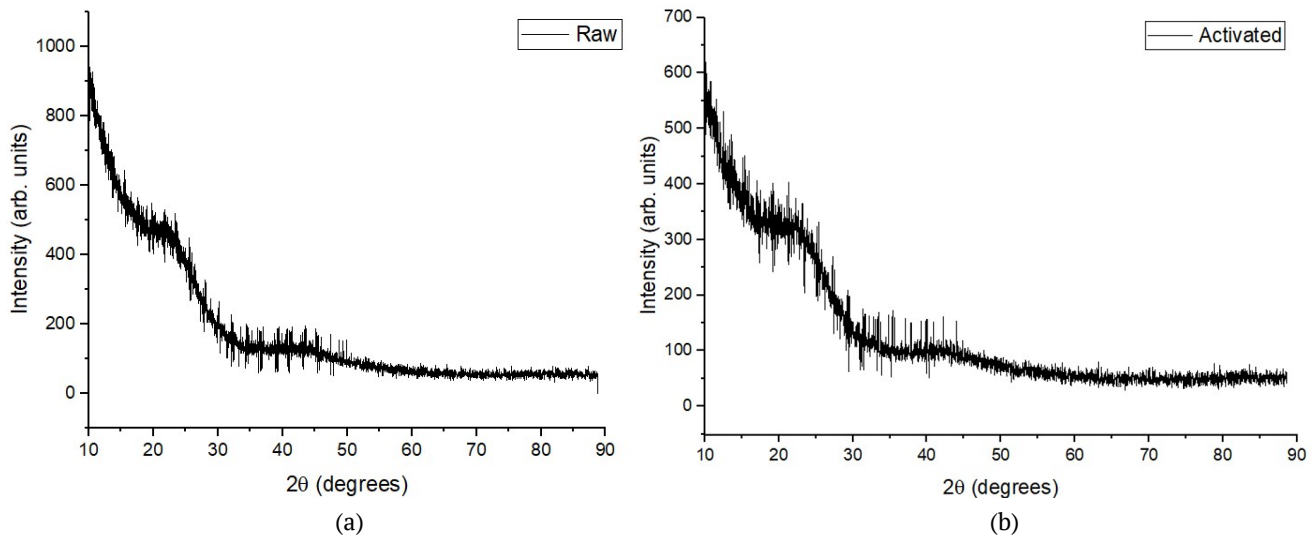


Figure 1. (a) Diffractometric pattern of Raw Char (b) Diffractometric pattern of Activated Char

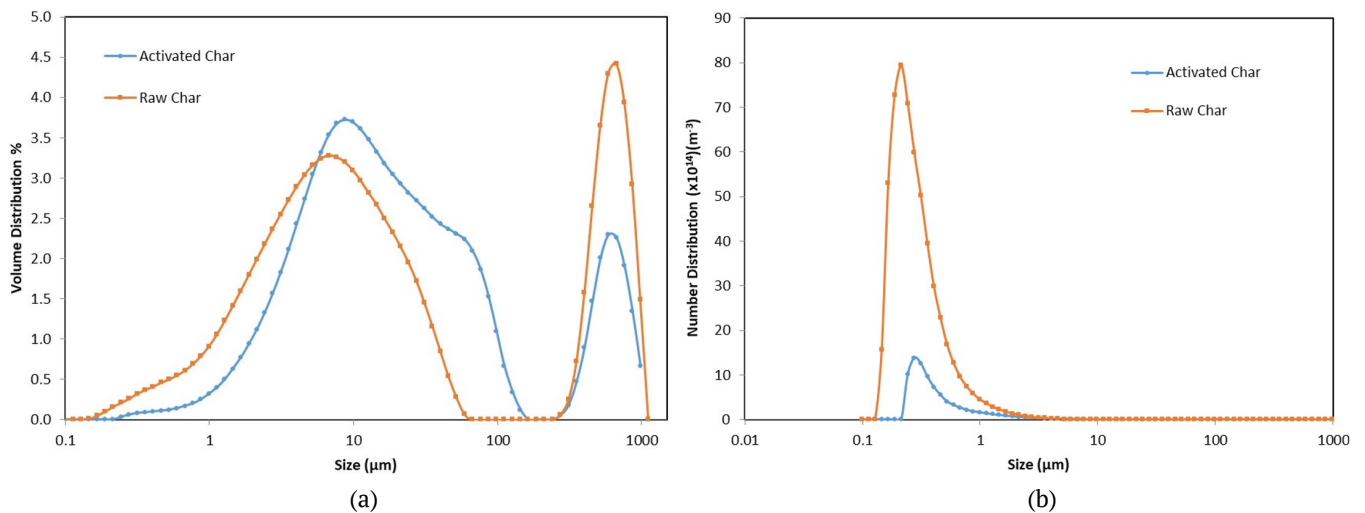


Figure 2. (a) Particle size analysis of Morula based Biochar - Volume Distribution (b) Particle size analysis of Morula based Biochar - Number Distribution

any changes in the diffraction pattern. The bump noticed between 20 and 30° $\sim 2\theta$ may be attributed to the scattering of x-rays which normally presents three or fewer halos in the diffractometric patterns (Bates et al., 2006).

Proximate Analysis (TGA)

Biochar was analyzed for moisture content, volatile matter and ash content. The main interest was the amount of fixed carbon in the char, it has been found that good chars have fixed carbon of over 75%. Moreover, it was found that the increase in pyrolytic temperature also increases the development of good char with the highest fixed carbon. From the **Table 1**, fixed carbon was found to be 80 and 84% at 600°C of pyrolysis temperature. This is because at higher temperatures the amount of lignin in the biomass is responsible for the formation of char. Lignin is a highly rigid substance which is resistant to thermal degradation, therefore can only be decomposed at higher temperatures, hence the higher the pyrolysis temperature the more the lignin is broken down to form char (Hernandez-Mena et al., 2014). The fixed carbon

Table 1. Proximate analysis of Morula based biochar

Name	Morula biochar
Moisture (%)	4.62
Volatile (%)	12.39
Volatile dry (%)	13.26
Ash (%)	2.47
Ash dry (%)	2.59
Fixed Carbon (%)	80.52
Fixed Carbon dry (%)	84.15

produced is due to the decomposition of the hydroxyl functional groups forming hydrogen and oxygen.

Particle Size Distribution (PSD)

The particle size volume and number distributions of both activated and raw biochars were determined and are shown in **Figure 2**. The bimodal curves are typical of an agglomeration process and show that particle agglomeration occurred during pyrolysis (Sithole et al., 2015). For raw biochar it was found that finer particles were concentrated at around 5.92 μm while larger particles ranged from 272 and 666 μm (**Figure 2**) and for

Table 2. Elemental composition from XRF

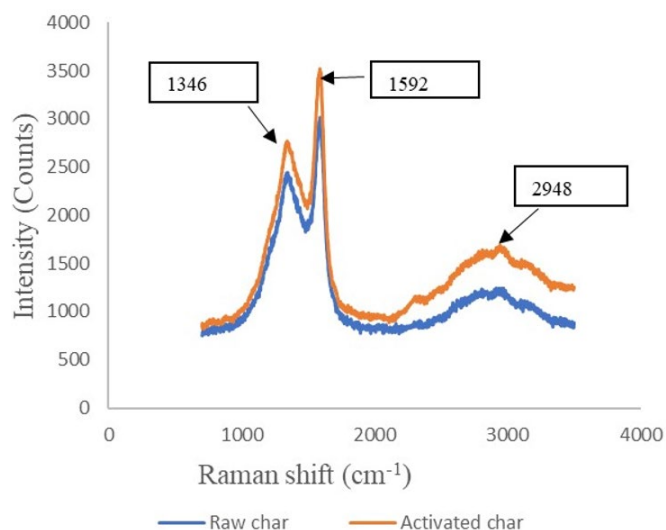
Elemental composition (wt.%)	Raw biochar		Activated biochar	
	Before	After	Before	After
Al	33.56	28.65	12.26	14.06
Si	3.78	7.51	5.44	4.98
P	1.37	2.44	0.94	0.71
S	1.52	2.69	1.52	2.61
Cl	0.32	0.65	60.82	50.13
K	38.62	14.67	0.92	0.58
Ca	16.76	10.46	7.53	6.51
Cr	0.85	0.79	0.97	0.98
Mn	1.12	1.19	1.34	1.28
Fe	1.70	24.49	7.50	13.52
Ni	0.00	0.55	0.00	0.00
Cu	0.26	0.28	0.65	0.34
Zn	0.08	5.59	0.04	0.27

NB: Before = Before Adsorption, After = After Adsorption

activated char the volume distribution shows that the finer particles were concentrated around 7.64 μm while larger particles ranged from 310-586 μm . From these two figures, it is seen that there is a higher proportion of larger sized particles in raw char as compared to activated char based on the volume distribution. This is an indication that activated char had few larger particles than raw char which might be due to size reduction during agitation when mixing with the acid. **Figure 2** shows that both chars had a higher number of finer particles of less than 1 μm with activated char having a modal size of 0.276 μm and raw char of 0.214 μm . The laser diffraction technique enables the calculation of the external surface area of the adsorbent particles by transforming the volume distribution to a number distribution and the surface area is thus calculated from the second moment (m_2 is equal to external surface area) (Ntuli and Lewis, 2009). It was found that the external surface area of activated char was 6.028 m^2/g and 11.83 m^2/g for raw char. Acid activation increases the surface functional groups in an adsorbent while decreasing the surface area hence the lower external surface area observed for activated char.

Chemical Composition (XRF)

Results from XRF shows that several metal elements are available on the biochar surface as presented in **Table 2**. Comparing the effect of acid activation of the biochar on the composition of the elements, it shows that Al, Ca and K reduced drastically. Since these are alkali metals, during acid activation with HCl the metal ions formed metal chlorides due to reaction with the acid. It was also found that Cl ions increased from 0.32% to 60.82% after activation which was expected due to addition of Cl ions to the char during activation. During adsorption of the raw biochar it was found that the concentration of the elements of interest for adsorption, Fe, Ni and Zn increased. Fe increased from 1.7% to 24.49%, Zn from 0.08% to 5.59% and Ni from 0 to 0.55%. This shows that these elements were adsorbed on the surface of the char, with Fe having the highest adsorption percentages. Other elements which experienced a change in concentration, include Ca and Al which dropped while S increased from 1.52% to 2.69%, and this may be attributed to the presence of sulphates in water which might have been adsorbed too.

**Figure 3.** Raman spectrum of raw and activated biochar

Functional Groups (Raman Spectroscopy)

One of the most important characteristics of an adsorbent is the surface functional groups, this was characterized using Raman spectrometer. **Figure 3** shows the available surface function groups in both raw and activated biochars. The spectrum indicates the presence of nitro group N=O (1346 cm^{-1}), aromatic ring C=C (1592 cm^{-1}) and carboxylic acid group O-H (2948 cm^{-1}). The aromatic peaks are normally present in chars which are pyrolyzed at higher temperatures of up to 400°C. This is because at lower temperatures of around 200 and 300°C only softer carbon components such as O-H functional groups are present. As the temperature is increased these groups break down leaving the hard carbon components which form stable chars with C=C and C=O bonds. This trend was observed by (Chen and Chen, 2009) and this explains the strong peak at 1592 cm^{-1} and a weaker peak at 2948 cm^{-1} since this biochar was carbonized at 600 °C. These groups are essential for increasing the oxygenated functional groups which are good adsorptive sites for metal ions. Both activated and raw chars depicted the same functional groups, with activated char having higher intensities for the peaks identified. This is because chemical activation increases the

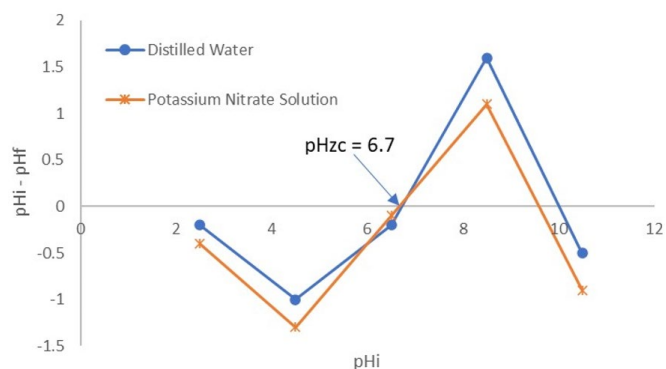


Figure 4. Point of Zero Charge for Morula based Biochar

acidic functional groups of the biochar which act as good adsorptive sites (Enaime et al., 2020).

Cation Exchange Capacity

It was found the activated biochar had a higher CEC of 33.257 meq/100 g than the raw biochar with 0.0962 meq/100 g as expected. This can be attributed to the fact that chemical activation increases porosity as well as the internal surface area of the chars hence the higher exchange of the Na cation. Thus, this enables adsorption of the cations into the exchangeable sites of the char. Increased CEC for acid activations was also observed by (Doğan and Alkan, 2003) on perlite biochars. The increase of CEC after activation process was also a result of the increase in oxygenated functional nitro group (1346 cm^{-1}) which means an increase in negative charges influences the uptake of Na ions (Nartey and Zhao, 2014).

Point of Zero Charge

The surface charge of an adsorbent is known to be a function of the solution pH and the point at which the net charge of the adsorbent is zero is known as the point of zero charge (pH_{ZC}) (Demirbas et al., 2009; Freitas et al., 2017). When the pH_{ZC} is lower than the solution pH, the surface charge of the adsorbent is then considered to be negative because as the surface charge decreases, the pH increases and this implies that metal adsorption will be higher (Chen et al., 1996). The pH_{ZC} of morula biochar was found to be 6.7 as shown in **Figure 4** and this suggests that at pH's below the pH_{ZC} the surface of the biochar is predominated by positive charges while at those greater than pH_{ZC} it is predominated by negative charges (Mohan and Gandhimathi, 2009). According to Kalemkiewicz and Soćo (2013), most metal ions start precipitating or forming metal hydroxide at pH's above 10 hence the pH_{ZC} was considered until pH 8.5 for this study. The presence of another pH_{ZC} at pH values greater than 8.5 is due to heterogeneity and presence of both carboxylic and nitro groups on the surface of the biochar.

Coal Wash Water Characterization

The coal wash water used for this study was characterised to determine the physicochemical characteristics of the water. The coal wash water samples before and after adsorption were analysed using standard methods as outlined in the Standard Methods for the Examination of Water and Wastewater (Eaton et al., 1998). The concentration levels of heavy metals, anions

Table 3. Coal wash water characterization

Heavy Metal	Concentration (ppm)
Iron	649.47
Zinc	661.24
Nickel	435.51
Copper	ND
Arsenic	ND
Lead	ND
Manganese	261.795
Anions	Concentration (ppm)
Chloride	102.790
Nitrate	676.90
Bromide	ND
Phosphate	ND
Fluoride	2.026
Sulphate	ND
Physical Parameters	
pH	8.38
Conductivity	1173 $\mu\text{S}/\text{cm}$
TDS	587 ppm
Dissolved Oxygen	3.85 ppm

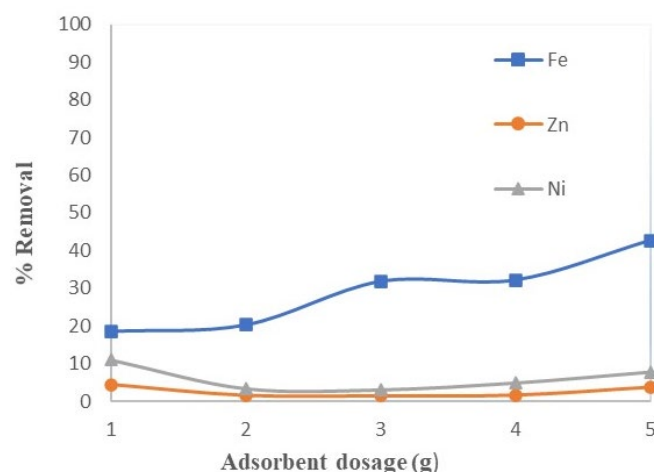


Figure 5. Percentage removals of Fe, Zn and Ni at concentrations of >600 mg/L for Fe and Zn and Ni at >400 mg/L using raw biochar at a pH of 5.8

and the physical parameters of coal wash water are presented in **Table 3**.

Effect of Adsorbent Dosage at Different Metal Ion Concentrations

Raw Biochar

From **Figure 5**, it was found that Fe percentage removals increased with increase in adsorbent dosage, with 18.56% using 1 g/100 mL and 42.64% using 5 g/100 mL of biochar. Zn and Ni portrayed a similar trend, they had the highest removals of 4.3% and 11.05% respectively with 1 g/100 mL and decreased as the dosage increased. However, there was a marginal increase in removal when using 5 g/100 mL. From **Figure 5**, it is evident that raw biochar removes these metal ions effectively at higher dosages. When using ion concentrations of 60 mg/L for Fe and Zn and 40 mg/L of Ni at char dosages of less than 1 g, it was observed that all the three ions had the highest removals compared to the previous experiment as indicated in **Figure 6**.

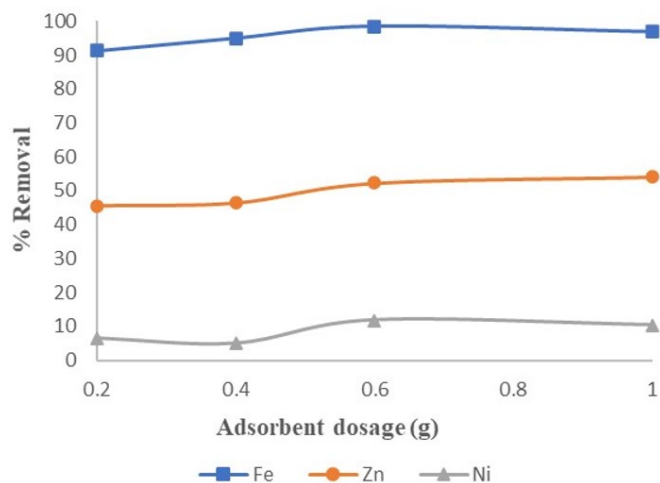


Figure 6. Percentage removals of Fe, Zn and Ni at concentrations of 60 mg/L for Fe and Zn and Ni at 40 mg/L using raw biochar at a pH of 5.8

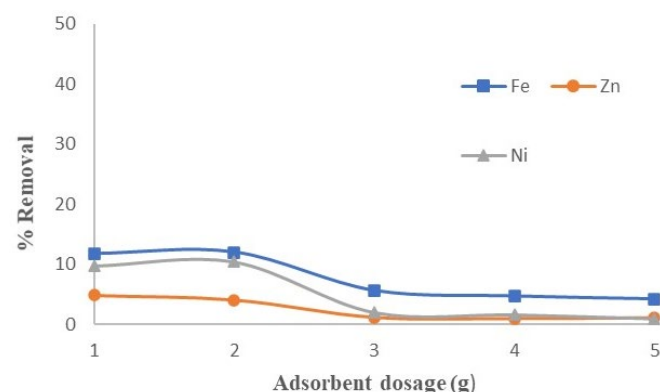


Figure 7. Percentage removals of Fe, Zn and Ni at concentrations of >600 mg/L for Fe and Zn and Ni at >400 mg/L using activated biochar at a pH of 5.8

Activated Biochar

When using activated biochar (**Figure 7**), all the ions had a similar trend: as the dosage increased the removal percentages dropped until they reached a constant point. Fe was preferentially removed using both raw and activated biochar and this might have been due to the ionic radius of these ions. The removal percentages were recorded as follows Fe > Ni > Zn and this corresponded to the ionic radii of these metal ions which are $0.7\text{\AA} < 0.72\text{\AA} < 0.74\text{\AA}$ respectively. It is known that the smaller the ionic radius the higher the adsorption capacity of the cation because the ion travels faster to adsorptive sites than the one with a large ionic radius (Gao et al., 2009). **Figure 8** shows that activated biochar works best at lower dosages. The overall lower removal percentages were attributed to high metal ion concentrations which might have led to saturation of adsorptive sites hence less ions adhered to the surface of the char. Realizing this trend, another experiment was done using lower dosages and lower metal ion concentrations.

Fe had removals of greater than 90% for both raw and activated biochar, Zn recorded more than 50% removals while Ni was the only one which had the lowest removals of less than 20% for both chars. The higher removals were due to lower metal ion concentrations, hence more adsorptive sites but less

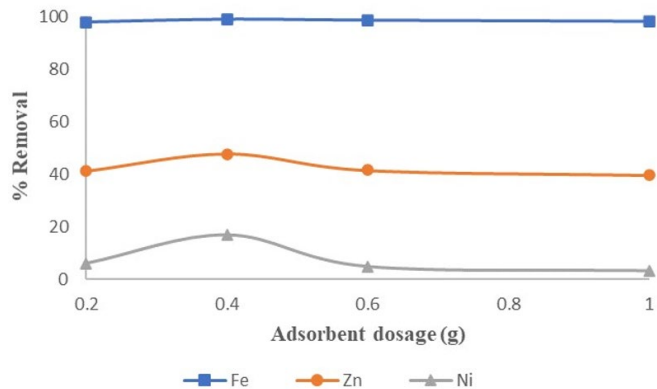


Figure 8. Percentage removals of Fe, Zn and Ni at concentrations of 60 mg/L for Fe and Zn and Ni at 40 mg/L using activated biochar at a pH of 5.8

heavy metal ions to adhere to the surface of the char. Several observations were made on the mechanisms of adsorption that might have occurred. For instance, it was postulated that cation exchange might have occurred during removal of heavy metals. Metal ions such as K^+ and Ca^{2+} were present in higher amounts on chars before adsorption. However, they decreased after adsorption as illustrated in **Table 2**, which shows that some have been removed from the char surface into the adsorbate, this trend was also observed by Yang et al. (2019). Furthermore, the presence of oxygenated functional groups on the surface of char might have led to electrostatic attraction between the metal ions and negatively charged oxygenated functional groups which led to ions being removed from the wastewater on to the surface of the biochar. In addition, the higher cation exchange capacity of activated char also contributed to the adsorption process (Xie et al., 2017).

CONCLUSION

Pyrolyzed morula shells can be used to remove heavy metals in wastewater. Acid modification of biochar increased its CEC and it was found that the point of zero charge for morula based biochar was 6.7 which is well lower than the pH of the solution hence making it act as a negative surface. Morula biochar presented an amorphous phase in the mineralogy study, and it also showed a higher fixed carbon content of more than 75% indicating that it is good for adsorption. Biochar had C=C, N=O and O-H surface functional groups which were responsible for the adsorption process by electrostatic attraction with the metal ions. The external surface area of raw and activated char was found to be 11.832 and 6.0286 m^2/g respectively. Elemental composition revealed the presence of several metal ions including K and Ca which played a role in cation exchange. It was noted that both raw and activated biochar removed Fe better than Zn and Ni mainly because of the ionic radius of the metal ions, with Fe having the smallest radius followed by Ni then Zn. Low dosages had a higher removal capacity at concentrations of 40 – 60 mg/L while higher dosages had lower removal capacities at concentrations of 400 – 600 mg/L. It can be concluded that morula shells could be used as a low-cost adsorbent in removing contaminants in wastewater.

Author contributions: All authors were involved in all the stages of this study while preparing the final version. They all agree with the results and conclusions.

Funding: No external funding is received for this article.

Declaration of interest: The authors declare that they have no competing interests.

Ethics approval and consent to participate: Not applicable.

Availability of data and materials: All data generated or analyzed during this study are available for sharing when appropriate request is directed to corresponding author.

REFERENCES

- Abdullah, E. J. (2013). Evaluation of surface water quality indices for heavy metals of Diyala River-Iraq. *Journal of Natural Sciences Research*, 3(8), 63-70.
- Ali, I. and Gupta, V. K. (2007). Advances in water treatment by adsorption technology. *Nature Protocols*, 1(6), 2661-2667. <https://doi.org/10.1038/nprot.2006.370>
- Bates, S., Zograf, G., Engers, D., Morris, K., Crowley, K. and Newman, A. (2006). Analysis of amorphous and nanocrystalline solids from their X-ray diffraction patterns. *Pharmaceutical Research*, 23(10), 2333-2349. <https://doi.org/10.1007/s11095-006-9086-2>
- Cao, Q., Huang, Z., Liu, S. and Wu, Y. (2019). Potential of Punica granatum biochar to adsorb Cu (II) in soil. *Nature*, 9(I), 1-13. <https://doi.org/10.1038/s41598-019-46983-2>
- Chen, B. and Chen, Z. (2009). Sorption of naphthalene and 1-naphthol by biochars of orange peels with different pyrolytic temperatures. *Chemosphere*, 76, 127-133. <https://doi.org/10.1016/j.chemosphere.2009.02.004>
- Chen, J., Yiaccoumi, S. and Blaydes, T. G. (1996). Equilibrium and kinetic studies of copper adsorption by activated carbon. *Separations Technology*, 6(2), 133-146. [https://doi.org/10.1016/0956-9618\(96\)00146-4](https://doi.org/10.1016/0956-9618(96)00146-4)
- Clesceri, L. S., Greenberg, A. E. and Eaton, A. D. (1998). Standard methods for the examination of water and wastewater (20th Ed.). Washington, DC: American Public Health Association.
- Demirbas, E., Dizge, N., Sulak, M. T. and Kobya, M. (2009). Adsorption kinetics and equilibrium of copper from aqueous solutions using hazelnut shell activated carbon. *Chemical Engineering Journal*, 148(2-3), 480-487. <https://doi.org/10.1016/j.cej.2008.09.027>
- Doğan, M. and Alkan, M. (2003). Removal of methyl violet from aqueous solution by perlite. *Journal of Colloid and Interface Science*, 267(1), 32-41. [https://doi.org/10.1016/S0021-9797\(03\)00579-4](https://doi.org/10.1016/S0021-9797(03)00579-4)
- Enaime, G., Baçaoui, A., Yaacoubi, A. and Lübken, M. (2020). Biochar for wastewater treatment-conversion technologies and applications. *Applied Sciences (Switzerland)*, 10(10), 1-29. <https://doi.org/10.3390/app10103492>
- Freitas, E. D., Carmo, A. C. R., Neto, A. F. A. and Vieira, M. G. A. (2017). Binary adsorption of silver and copper on Verde-lodo bentonite: Kinetic and equilibrium study. *Applied Clay Science*, 137, 69-76. <https://doi.org/10.1016/j.clay.2016.12.016>
- Gao, Z., Bandosz, T. J., Zhao, Z., Han, M. and Qui, J. (2009). Investigation of factors affecting adsorption of transition metals on oxidized carbon nanotubes. *Journal of Hazardous Materials*, 167(1-3), 357-365. <https://doi.org/10.1016/j.jhazmat.2009.01.050>
- Hayashi, J., Kazehaya, A., Muroyama, K. and Watkinson, A. P. (2000). Preparation of activated carbon from lignin by chemical activation. *Carbon*, 38(13), 1873-1878. [https://doi.org/10.1016/S0008-6223\(00\)00027-0](https://doi.org/10.1016/S0008-6223(00)00027-0)
- Hernandez-Mena, L. E., Pecora, A. A. B. and Beraldo, A. L. (2014). Slow pyrolysis of bamboo biomass: Analysis of biochar properties. *Chemical Engineering Transactions*, 37, 115-120. <https://doi.org/10.3303/CET1437020>
- Kalembkiewicz, J. and Soc, E. (2013). Adsorption of nickel (II) and copper (II) ions from aqueous solution by coal fly ash. *Journal of Environmental Chemical Engineering*, 1, 581-588. <https://doi.org/10.1016/j.jece.2013.06.029>
- Kapur, M. and Mondal, M. K. (2014). Competitive sorption of Cu (II) and Ni (II) ions from aqueous solutions: Kinetics, thermodynamics and desorption studies. *Journal of the Taiwan Institute of Chemical Engineers*, 45(4), 1803-1813. <https://doi.org/10.1016/j.jtice.2014.02.022>
- Lekgoba, T., Ntuli, F. and Falayi, T. (2020). Application of coal fly ash for treatment of wastewater containing a binary mixture of copper and nickel. *Journal of Water Process Engineering*, 40(November 2020), 101822. <https://doi.org/10.1016/j.jwpe.2020.101822>
- Malaviya, P. and Singh, A. (2011). Physicochemical technologies for remediation of chromium-containing waters and wastewaters. *Critical Reviews in Environmental Science and Technology*, 41(12), 1111-1172. <https://doi.org/10.1080/10643380903392817>
- Mohan, S. and Gandhimathi, R. (2009). Removal of heavy metal ions from municipal solid waste leachate using coal fly ash as an adsorbent. *Journal of Hazardous Materials*, 169, 351-359. <https://doi.org/10.1016/j.jhazmat.2009.03.104>
- Nartey, O. D. and Zhao, B. (2014). Biochar preparation, characterization, and adsorptive capacity and its effect on bioavailability of contaminants: An overview. *Advances in Materials Science and Engineering*, 2014, 715398. <https://doi.org/10.1155/2014/715398>
- Ntuli, F. and Lewis, A. E. (2009). Kinetic modelling of nickel powder precipitation by high-pressure hydrogen reduction. *Chemical Engineering Science*, 64(9), 2202-2215. <https://doi.org/10.1016/j.ces.2009.01.026>
- Sen, T. K. and Gomez, D. (2011). Adsorption of zinc (Zn²⁺) from aqueous solution on natural bentonite. *DES*, 267(2-3), 286-294. <https://doi.org/10.1016/j.desal.2010.09.041>
- Sharma, S. and Bhattacharya, A. (2017). Drinking water contamination and treatment techniques. *Applied Water Science*, 7(3), 1043-1067. <https://doi.org/10.1007/s13201-016-0455-7>
- Sithole, T., Ntuli, F. and Falayi, T. (2015). The removal of Ni & Cu from a mixed metal system using Sodium borohydride as a reducing agent. *South African Journal of Chemical Engineering*, 20(1), 16-29.

- Wynberg, R., Cribbins, J., Lombard, C. and Mander, M. (2002). Knowledge on *Sclerocarya birrea* subsp. *caffra* with emphasis on its importance as a non-timber forest product in South and southern Africa: A Summary. *South Africa Forestry Journal*, 196(1), 67-77. <https://doi.org/10.1080/20702620.2002.10434589>
- Xie, R., Jin, Y., Chen, Y. and Jiang, W. (2017). The importance of surface functional groups in the adsorption of copper onto walnut shell derived activated carbon. *Water Science and Technology: A Journal of the International Association on Water Pollution Research*, 76(11-12), 3022-3034. <https://doi.org/10.2166/wst.2017.471>
- Yang, X., Wan, Y., Zhen, Y., He, F., Yu, Z., Huang, J., Wang, H., Ok, Y. S., Jiang, Y. and Gao, B. (2019). Surface functional groups of carbon-based adsorbents and their roles in the removal of heavy metals from aqueous solutions: A critical review. *Chemical Engineering Journal*, 366, 608-621. <https://doi.org/10.1016/j.cej.2019.02.119>